Asymmetric Distyrylpyridinium Dyes as Red-Emitting Fluorescent Probes for Quadruplex DNA

Xiao Xie, Bina Choi, Eric A Largy, Régis Guillot, Anton Granzhan, Marie-Paule Teulade-Fichou

CHEMISTRY
A EUROPEAN JOURNAL

FULL PAPER

DOI: 10.1002/chem.200((will be filled in by the editorial staff))

Asymmetric Distyrylpyridinium Dyes as Red-Emitting Fluorescent Probes for Quadruplex DNA

Xiao Xie,[a] Bina Choi,[a,b] Eric Largy,[a] Régis Guillot,[c] Anton Granzhan,[a] and Marie-Paule Teulade-Fichou*[a]

Abstract: The interactions of three cationic distyryl dyes, namely 2,4-bis(4-dimethylaminostyryl)-1-methylpyridinium (**1a**), its derivative with a quaternary aminoalkyl chain (**1b**), and the symmetric 2,6-bis(4-dimethylaminostyryl)-1-methylpyridinium (**2a**), with several quadruplex and duplex nucleic acids were studied with the aim to establish the influence of the geometry of the dyes on their DNA-binding and DNA-probing properties. The results from spectrofluorimetric titrations and thermal denaturation experiments provide evidence that the asymmetric (2,4-disubstituted) dyes **1a** and **1b** bind to quadruplex DNA structures with a near-micromolar affinity and a fair selectivity with respect to double-stranded DNA [K_a(G4) / K_a(ds) = 2.5–8.4]. At the same time, the fluorescence of both dyes is selectively increased in the presence of quadruplex DNAs (more than 80–100-fold in the case of human telomeric quadruplex), even in the presence of excess competing double-stranded DNA. This optical selectivity allows for these dyes to be used as quadruplex-DNA-selective probes in solution and stains in polyacrylamide gels. In contrast, the symmetric analogue **2a** displays a strong binding preference for double-stranded DNA [K_a(ds) / K_a(G4) = 40–100), presumably due to binding in the minor groove. In addition, **2a** is not able to discriminate between quadruplex and duplex DNA, as its fluorescence is increased equally well (20–50-fold) in the presence of both structures. This study emphasizes and rationalizes the strong impact of subtle structural variations on both DNA-recognition properties and fluorimetric response of organic dyes.

Keywords: styryl dyes • fluorescent probes • DNA recognition • quadruplex DNA • gel electrophoresis

Introduction

Single-stranded nucleic acids containing repeats of guanine bases are known to adopt non-canonical four-stranded secondary structures called G-quadruplexes, composed of several stacks of guanine quartets held together by hydrogen bonds and metal cations (usually K^+ or Na^+) sandwiched between the quartets.[1] In spite of being well-studied *in vitro*, the evidence for the presence of quadruplex structures *in vivo* remains mainly indirect, but is currently supported by a growing wealth of biochemical and molecular genetics data.[2] In this context, the question of direct visualization of quadruplex structures (e.g. by fluorescence microscopy) becomes highly important, and the search for fluorescent probes capable of signaling of the presence of quadruplex DNA represents a timely and challenging task.[3] Nonetheless, one should bear in mind that putative quadruplex DNA structures *in vivo* are embedded into a massive excess of the prevailingly double-stranded genome, and their selective detection can be made possible by probes that either (i) have an overwhelmingly higher binding affinity for quadruplex over duplex DNA or (ii) bind to these two structures via different binding modes, resulting in different changes of fluorescence properties. Therefore, while one strategy for the development of quadruplex-DNA-selective fluorescent probes relies on the introduction of fluorophore units into highly quadruplex-selective ligand scaffolds (e.g. the BODIPY-labeled analogues of telomestatin[4] and pyridodicarboxamide),[5] another seeks for environmentally sensitive fluorescent probes capable of discriminating between the two related DNA structures. Successful examples of the latter strategy include *N*-methylmesoporphyrin IX,[6] the benzothiazole-substituted benzofuroquinolinium dye whose fluorescence increases ~300–350-fold in the presence of quadruplex DNA but only ~40–50-fold in the presence of the duplex,[7] as well as the merged pyridodicarboxamide–thiazole orange conjugate (PDC-M-TO), whose fluorescence increases eight times more in the presence of quadruplex DNA than in the presence

[a] X. Xie, Dr. E. Largy, Dr. A. Granzhan, Dr. M.-P. Teulade-Fichou
CNRS UMR176, Institut Curie, Centre de Recherche
91405 Orsay, France
E-mail: mp.teulade-fichou@curie.fr

[b] B. Choi
Exchange student from the Massachusetts Institute of Technology
Cambridge MA, USA

[c] Dr. R. Guillot
CNRS UMR8182, Institut de Chimie Moléculaire et des Matériaux d'Orsay, Université Paris-Sud XI
91405 Orsay, France

Supporting information for this article is available on the WWW under http://www.chemeurj.org/ or from the author.

of duplex counterpart.[8] The two latter probes are based on the fluorophore of thiazole orange, a DNA-sensitive cyanine dye whose selectivity to quadruplex structures is deliberately increased upon fusion with heterocyclic fragments.

Besides cyanine dyes, styryl (or arylvinyl) dyes represent an important class of functional dyes with applications as optical recording media, laser dyes, optical sensitizers and fluorescent probes in biomedical applications.[9,10] Recently, screening of styryl dye libraries led to the discovery of fluorescent probes for DNA, RNA, β-amyloid peptide, chemotrypsin, heparin and other bioanalytes.[11] Moreover, symmetric distyryl dyes based on 2,6-pyrydinium[12] and 2,8-quinolizinium[13] scaffolds have been established as fluorescent "light-up" probes for double-stranded DNA, useful for live-cell imaging. On the other hand, the symmetric dicationic dye 3,6-bis(1-methyl-4-vinylpyridium)carbazole (BMVC) was recently developed as a fluorescent "light-up" probe for nucleic acids, able to discriminate between duplex and quadruplex structures due to the differences in changes to emission maxima and fluorescence lifetimes upon binding. This was tentatively applied to the detection of G-quadruplex structures in cells.[14]

The 2,4- and 2,6-bis(4-dimethylaminostyryl)-1-methyl-pyridinium dyes (**1a** and **2a**, respectively) were initially synthesized in the 1930's,[15] and have recently gained attention due to their interesting non-linear optical properties[16] and antitumor activity.[17] However, their binding to nucleic acids has not been investigated, thus far. Herein, we report on the studies of interaction of the distyryl dye **1a**, its cationic-chain derivative **1b**, and **2a** with selected double-stranded and quadruplex DNA structures. Furthermore, we report on the accompanying changes in the spectroscopic properties of the dyes, aiming to develop fluorescent probes capable of discriminating among these DNA structures.

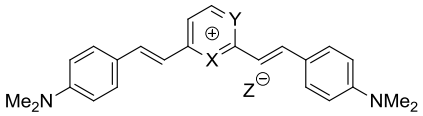

1a: X = CH, Y = NMe, Z = I

1b: X = CH, Y = $N(CH_2)_4N^+Et_3$ Br^-, Z = Br

2a: X = NMe, Y = CH, Z = I

Results

Synthesis and structural analysis of dyes

The dyes **1a** and **2a** were synthesized via condensation of 1,2,4- and 1,2,6-trimethylpyridinium iodides, respectively, with 4-(dimethylamino)benzaldehyde according to the established protocols; their characterization data were in agreement with the literature.[15–16,18] The dye **1b**, a cationic-chain derivative of **1a**, was synthesized in an analogous way from the 2,4-dimethyl-1-(4-(triethylammonio)-butyl)pyridinium dibromide **3** (see Experimental Section), and gave satisfactory ^{1}H and ^{13}C NMR, MS and elemental analysis data. The structures of compounds **1a** and **2a** in the solid state were studied by single-crystal X-ray diffraction analysis using crystals obtained in MeCN–H_2O, and revealed significant differences with respect to the mutual orientation of styryl substituents in the dye cations (Figure 1). Thus, compound **1a** crystallized in the space group *C*2/*c* and revealed the presence of quasi-planar cations (r.m.s. deviation from planarity of 0.37 Å for non-H atoms) with an angle of 108° between the axes of 4-(dimethylamino)phenyl substituents and a distance of 15.6 Å between the terminal nitrogen atoms. In contrast, the cations of **2a** in the solid state (space group: $P2_1/c$) adopt an extended conformation with an angle of 132° between the axes of 4-(dimethylamino)phenyl substituents and a distance of 17.6 Å between the terminal nitrogen atoms. Notably, these differences in conformations are due to the position of the methyl substituent, which forces the *s-trans* conformation of the adjacent bond in position 2 of the pyridinium ring; the two conformations can be conceptually interconverted by rotation of the styryl substituent about this bond (C6–C7 in Figure 1, b).

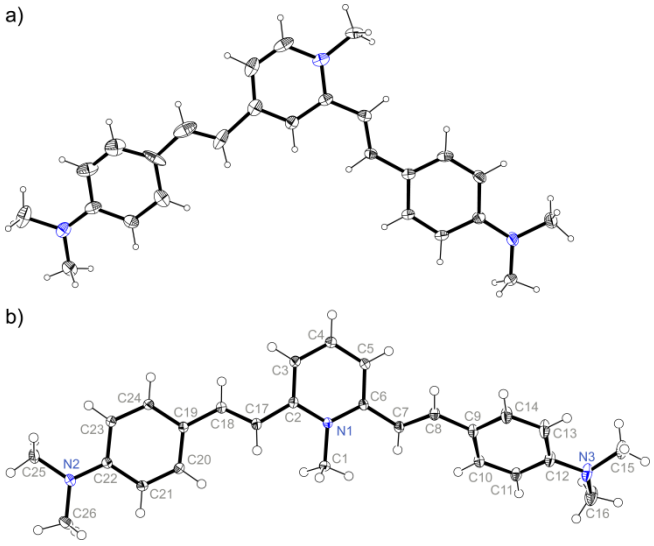

Figure 1. Structures of the dyes **1a** (a) and **2a** (b) in the solid state. ORTEP ellipsoids are drawn at the 20% (**1a**) or 50% (**2a**) probability level; iodide counter-ions are omitted for clarity. Atom numbering is arbitrary.

In contrast to the cations of **1a**, which were essentially planar, in **2a** the styryl substituents were significantly turned out of the plane of the pyridinium ring (torsion angles C5–C6–C7–C8 and C3–C2–C17–C18 of 30.8° and 25.5°, respectively), leading to the r.m.s. deviation from planarity of 4.14 Å for non-H atoms. Although quite unexpected when considering the less efficient conjugation of the double bonds, this non-planarity can be attributed to the peculiar packing of **2a** in the crystal, with two cations stacking via an overlap of only one of the two styryl moieties of each cation, in an anti-parallel fashion (Supporting Information, Figure S1).

Spectral properties of free dyes and quantum chemical calculations

In buffered aqueous solutions of relatively high ionic strength (10 mM $LiAsMe_2O_2$, 100 mM KCl, pH 7.2), both dyes displayed broad absorption bands, blue-shifted by ~30 nm with respect to the bands observed in methanol (Figure 1; cf. Table S1, Supporting Information, for the detailed data). In addition, the spectrum of **1a** (at a concentration of 10 μM) displays an additional red-shifted peak (λ_{max} = 618 nm), whose relative intensity increases at low temperatures (Supporting Information, Figure S2), which is characteristic of the formation of J-aggregates.[19] In contrast, the absorption spectra of **1b** and **2a** were essentially unchanged between 5 and 95 °C, evidencing that these dyes have a lower propensity to aggregate in these conditions. All three compounds are almost non-fluorescent in aqueous solutions (ϕ_f = 0.3–1.4 ×10^{-4}), with very

weak and broad fluorescence bands in the red region of spectrum ($\lambda_{em} \approx 680$ nm for **1a** and **1b**; $\lambda_{em} \approx 650$ nm for **2a**) and thus display remarkable Stokes shifts of ~200 nm for **1a–b** and ~180 nm for **2a**. The low fluorescence of the distyryl dyes in aqueous solution is in agreement with the literature data (**1a**: $\phi_f = 0.002$, **2a**: $\phi_f = 0.0004$ in MeOH).[20]

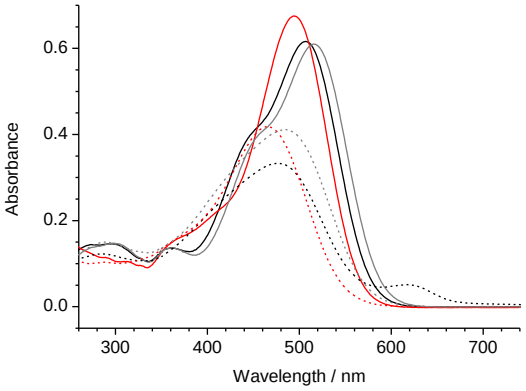

Figure 2. Absorption spectra (c = 10 µM) of dyes **1a** (black), **1b** (grey) and **2a** (red) in methanol (solid lines) and in aqueous buffer (10 mM $LiAsMe_2O_2$, 100 mM KCl buffer, pH 7.2; dashed lines).

Taken together, these spectral features (i.e. broad, solvatochromic long-wavelength absorption bands, large Stokes shift) are characteristic of donor–acceptor systems exhibiting internal charge transfer upon excitation. In this regard, the absorption maxima of the asymmetric dyes **1a** and **1b** are red-shifted with respect to the symmetric analogue **2a**, which gives evidence for a more pronounced charge-transfer interaction in **1a** and **1b.**

To get insight into the nature of electronic transitions in distyryl dyes, we performed density functional theory (DFT) calculations with a hybrid exchange-correlation CAM-B3LYP functional, well-suited for the treatment of charge-transfer phenomena,[21] and a D95V basis set. The ground-state geometry optimization performed at this level of theory indicated deviation of planarity in cation of **2a**, as both styryl substituents were turned by 26° with respect to the plane of the central pyridinium ring; in contrast, the ground-state-optimized structure of **1a** was planar, fully in accordance with the single-crystal X-ray data. The time-dependent (TD-DFT) calculations at the same level of theory indicated that in both dyes, the low-energy electronic transition involved the HOMO → LUMO transition as a major, but not the sole, contribution (CI coefficient of 0.65 in both cases). The energies of vertical transitions from the TD-DFT calculations (480 nm and 465 nm for **1a** and **2a**, respectively) were in excellent agreement with the experimental data (cf. Table 1), validating the choice of the computational method. Further analysis of the electronic density in the ground and first excited states of **1a** and **2a** (Figure 3) confirmed the charge-transfer character of their low-energy electronic transitions: the excitation is accompanied by a reorientation (in the case of **1a**) or a large increase (in the case of **2a**) of dipole moments of the dye cations. Upon excitation, the electron density is transferred from the lateral dimethylaminostyryl substituents to the positions 1,2,4 (**1a**) or 1,2,6 (**2a**) of the central pyrydinium ring of the dyes.

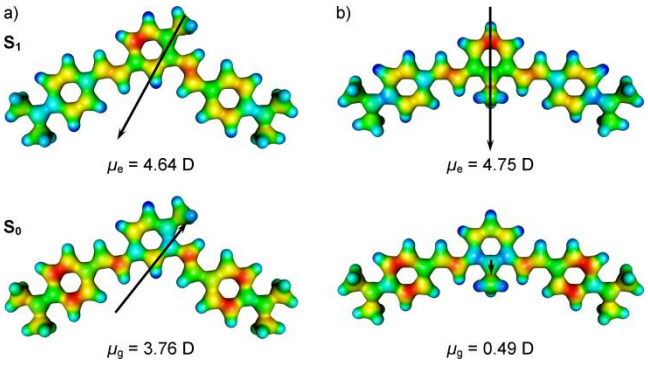

Figure 3. TD-DFT-derived charge distribution (isosurface value of 0.05) of the electronic ground (S_0) and first excited (S_1) states of the cations **1a** (a) and **2a** (b) in vacuo (negative: red, positive: blue). The arrows represent the orientation and magnitude of calculated dipole moments in the corresponding electronic states.

The quantum chemical calculations also help explain the differences in aggregation behavior of **1a** and **2a** in aqueous medium. The large static dipole moment of the dye **1a** (μ_g = 3.76 D) favors the intermolecular interactions between the dye cations, leading to aggregation, presumably in an antiparallel fashion as observed in the solid state (cf. Figure S1, Supporting Information), whereas in the case of **2a**, its small ground-state dipole moment (μ_g = 0.49 D) is not sufficient for aggregation at the employed concentrations.

Spectroscopic studies of interaction with duplex and quadruplex DNA

Spectrophotometric titrations. The interactions of the dyes **1a–b** and **2a** with nucleic acids were initially qualitatively studied by UV–Vis absorption titrations with calf thymus DNA (ct DNA) and c-kit2 and as representative duplex and quadruplex nucleic acids (Table 2). The changes in absorption spectra observed during the titrations are shown on Figure 4.

Table 1. Nucleic acids used in this work.[a]

Acronym	Sequence (5′ → 3′)	Remarks (topology)
	quadruplex DNAs[b]	
22AG	AGGGTTAGGGTTAGGGTTAGGG	human telomeric ([3 + 1] forms 1 and 2)
c-myc	TGAGGGTGGGTAGGGTGGGTAA	c-myc promoter (parallel)
c-kit87up	AGGGAGGGCGCTGGGAGGAGGG	c-kit1 promoter (snap-back parallel)
c-kit2	GGGCGGGCGCGAGGGAGGGG	modified c-kit2 promoter (parallel)
TBA	GGTTGGTGTGGTTGG	thrombin-binding aptamer (antiparallel)
	duplex DNAs[c]	
ct DNA	genomic highly polymerized	calf thymus DNA
ds-lac	$(GAATTGTGAGCGCTCACAATTC)_2$	symmetric lac operator

DrewAT	(CGCG<u>AAATTT</u>CGCG)$_2$	AT-enhanced Dickerson–Drew duplex

[a] Concentration units used in this work refer to the molar concentration of oligonucleotide strands in the case of quadruplexes, double strands in the case of duplexes, and base pairs (bp) in the case of ct DNA. [b] The guanine bases participating in formation of G-quartets are underlined. [c] The putative minor-groove-binding sites are double-underlined.

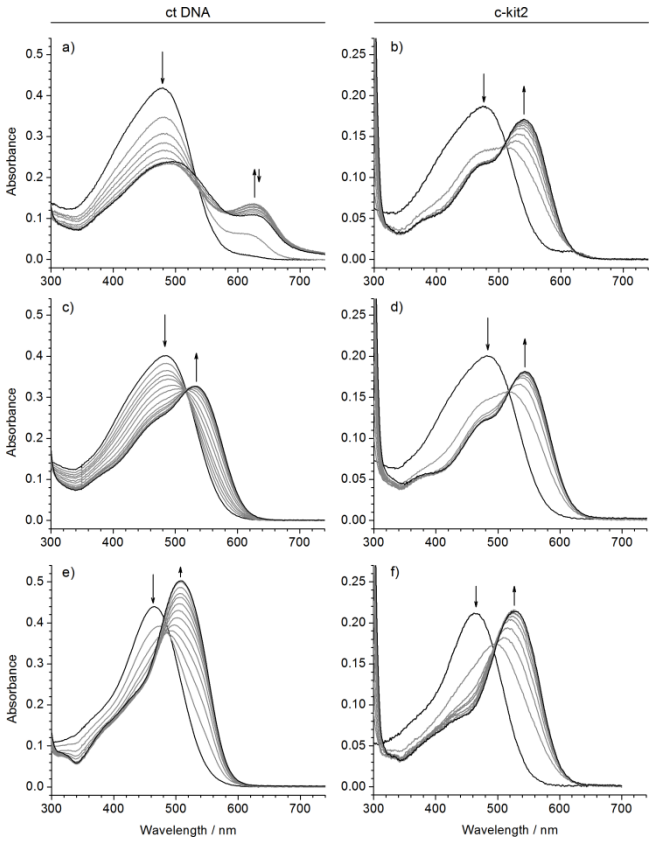

Figure 4. Spectrophotometric titrations of the dyes **1a** (a–b), **1b** (c–d) and **2a** (e–f) with ct DNA (0 to 130 μM bp) and c-kit2 quadruplex (0 to 25 μM). The concentration of the dyes was 10 μM (for titrations with ct DNA) or 5 μM (for titrations with c-kit2) in 10 mM $LiAsMe_2O_2$, 100 mM KCl buffer, pH 7.2. The initial and final spectra are drawn black; the arrows indicate the changes in absorption spectra observed during the titrations.

Remarkably, the dyes exhibited different behaviors upon interaction with ct DNA. The dye **1a** interacted with ct DNA with significant enhancement of the absorption band of the J-aggregate (λ_{max} = 625 nm), which, in the absence of ct DNA, was present as a small shoulder on the red edge of the main absorption band (Figure 4, a). Moreover, the position of the J-aggregate band in the presence of ct DNA was red-shifted by 7–8 nm compared to that observed in the solutions of **1a** alone at low temperatures (cf. Table S1 and Figure 1 showing spectra of free dye **1a**), which gives evidence of external dye aggregation templated by duplex DNA. The main absorption band of the dye prevailed even at high DNA loading (phosphate/dye ratio > 20 at the end of titration) and underwent almost no spectral shift. This indicates that, in the case of **1a**, the DNA-bound J-aggregates of the dye are in equilibrium with the unbound monomeric form in solution. However, when titration was performed at lower concentration of **1a** (5 μM), no increase of the J-aggregate band was observed (Figure S3, Supporting Information). In contrast, the dyes **1b** and **2b** both showed interaction of the monomeric form with ct DNA, as evidenced by the red shift (by 40–50 nm) of their absorption bands, accompanied by hypochromic (**1b**, Figure 4, c) or hyperchromic (**2a**, Figure 4, e) effects.

The interactions of all three dyes with quadruplex DNA (Figure 4, b,d,f) were characterized by the strong reduction of absorption bands of the free dyes and the formation of new, narrower bands red-shifted by 60–65 nm. In the case of **1a** and **1b**, the new bands showed reduced intensity (hypochromic effect) and a sharper vibronic shoulder on the blue edge of the absorption band. Of note, the red shift of the absorption bands of the dyes was larger in the case of quadruplex DNA, pointing out to differences in the dye-binding sites (geometry, polarity) in duplex and quadruplex DNA.

Fluorimetric titrations. We investigated the changes in fluorescence of the distyryl dyes in the presence of a larger panel of quadruplex DNA structures, as well as two double-stranded oligonucleotides featuring short sequential A-runs, well-suited for accommodation of groove-binding ligands (DrewAT: 5′-AAATTT-3′, ds-lac: 2 × 5′-AATT-3′), and highly polymerized ct DNA (Table 1). In most cases, the fluorescence of the dyes, very low in aqueous solutions, increased upon the addition of DNA; the representative titrations of the dye **1a** with quadruplex (22AG) and duplex (ds-lac) oligonucleotides are shown in Figure 5. However, the degree of fluorescence enhancement revealed strong differences between the quadruplex and duplex DNA, as well as among the dyes (Figure 6). Thus, the fluorescence of both **1a** and **1b** was largely increased upon addition of the human telomeric quadruplex 22AG (~110-fold and ~80-fold at saturation, respectively). The quadruplex structures from oncogenes (c-myc, c-kit87up, c-kit2) induced weaker enhancement of fluorescence (40–60-fold at saturation for both dyes), whereas the TBA quadruplex induced an even smaller effect (~20-fold enhancement) in all cases. In contrast, the addition of duplex DNA (ds-lac, DrewAT, ct DNA) resulted in a much smaller fluorescence enhancement for both **1a** and **1b** (less than 20-fold). In particular, almost no or slight increase of fluorescence was observed upon titration of ct DNA, ds-lac and DrewAT to **1a** (Figure 6, a). A very similar behavior was noted for **1b**: the addition of both ct DNA and short duplexes led to low fluorescence enhancement, compared to that induced by quadruplexes (Figure 6, b). Again, TBA was rather inefficient to increase the dye fluorescence.

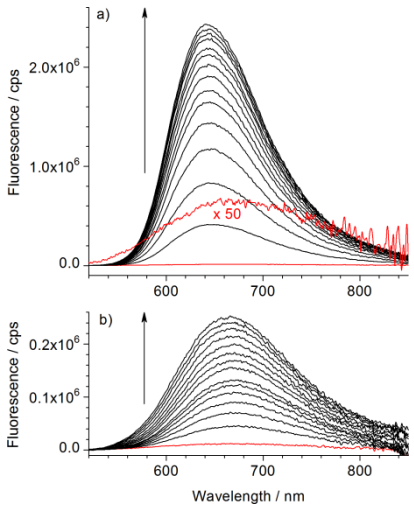

Figure 5. Spectrofluorimetric titrations of the dye **1a** (2.5 μM) with a) 22AG quadruplex and b) ds-lac duplex DNA (0 to 17 μM each). Excitation wavelength λ_{ex} = 510 nm. The red lines represent the spectrum of the dye in the absence of DNA; the arrows indicate the changes in fluorescence spectra observed during the titrations.

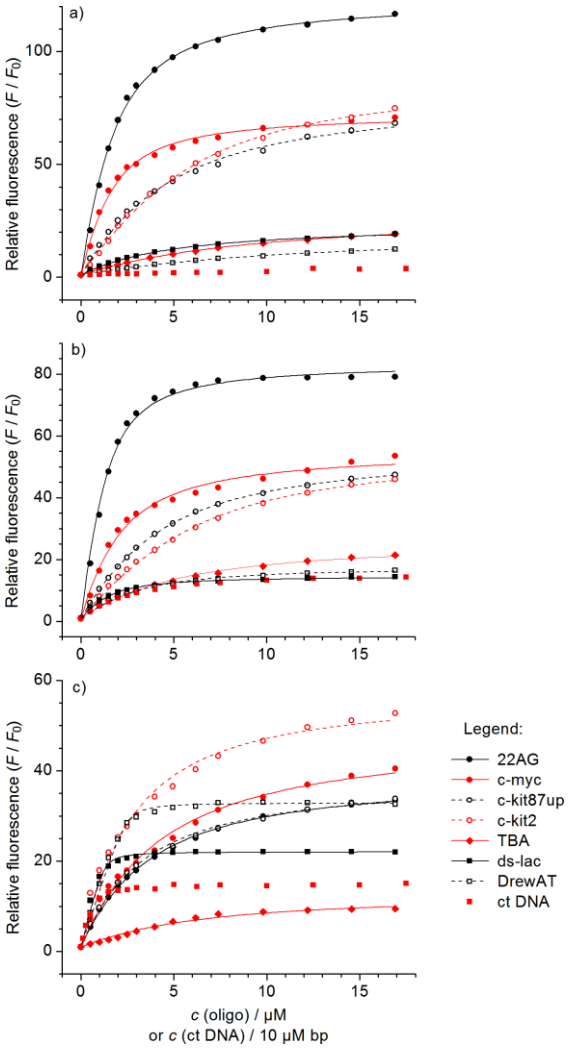

Figure 6. Spectrofluorimetric titrations, presented as relative increase of integral fluorescence (F / F_0), of various DNA structures (see legend) to the dyes **1a** (a, λ_{ex} = 510 nm), **1b** (b, λ_{ex} = 519 nm) and **2a** (c, λ_{ex} = 493 nm). Concentration of the dyes was 2.5 μM in 10 mM $LiAsMe_2O_2$, 100 mM KCl buffer, pH 7.2. The lines represent fitting to the independent-site model (see Experimental Part) using the parameters given in Table 3. The concentration of ct DNA is presented such that the total concentration in phosphate is comparable to oligonucleotides.

Interestingly, both **1a** and **1b** were able to discriminate between quadruplex (22AG, c-myc, c-kit87up, c-kit2) and duplex DNA not only by the magnitude of the "light-up" effect (enhancement of fluorescence), but also by the position of emission maxima in fluorescence spectra, which is blue-shifted by 15–20 nm in quadruplexes as compared to duplexes and TBA (cf. Figure 5). This is reminiscent of the behavior of BMVC and other vinylcarbazoles.[10d,14]

In contrast to the asymmetric dyes, the fluorimetric response of the symmetric analogue **2a** was found to poorly discriminate between quadruplex and duplex structures (Figure 6, c). The strongest "light-up" effect was observed in the presence of c-kit2 quadruplex (fluorescence enhancement by a factor of > 50 at saturation), while in the presence of other quadruplex and duplex structures, the enhancement factor was between 20 and 40, again with an exception for TBA (~10). Also, the positions of emission maxima of **2a** were less sensitive in distinguishing between the nucleic acids (λ_{max} = 623–629 nm for duplexes and 626–639 nm for quadruplexes). The analysis of binding isotherms revealed the rapid saturation of binding of **2a** to duplex DNA and the absence of saturation even at large excess (> 7 molar equivalents) of quadruplex DNA.

To estimate the binding affinity and stoichiometry of the distyryl dyes to duplex and quadruplex DNAs, the binding isotherms from fluorimetric titrations were analyzed according to the independent-site model.[22] The results presented in Table 2 reveal several interesting regularities: (i) **1a** binds to quadruplexes 22AG, c-myc and c-kit87up with a more or less similar affinity falling in the range 0.31–0.55 × 10^6 M^{-1} and an apparent 2 : 1 to 1 : 1 stoichiometry (dye : DNA). This stoichiometry was independently confirmed by continuous variation analysis (Figure S4). (ii) Surprisingly, binding of **1a** to c-kit2 is better described by a 1 : 2 model (i.e. one molecule of dye per two quadruplexes), which is also apparent from the corresponding Job plot (Supporting Information, Figure S4). (iii) The affinity of **1a** for TBA (K_a = 0.13 × 10^6 M^{-1}) is significantly lower compared to other quadruplexes. (iv) **1a** shows very low affinity for the two duplexes (K_a = 0.12 and 0.09 × 10^6 M^{-1}, respectively). (v) Dye **1b** exhibits the same trends as **1a** in terms of stoichiometry, but with higher affinity for the 22AG quadruplex (K_a = 0.93 × 10^6 M^{-1}) and both duplexes (K_a = 0.67–0.68 × 10^6 M^{-1}). (vi) In contrast, **2a** has a very high affinity to duplexes ds-lac and particularly DrewAT (K_a = 8.91 and 18.4 × 10^6 M^{-1}, respectively) and a lower affinity for all quadruplexes (0.17–0.24 × 10^6 M^{-1}). (vii) All three dyes show a 2 : 1 binding stoichiometry with ds-lac and 1 : 1 with DrewAT, in accordance with the number of AT-tracts defining the minor-groove sites which are likely to accommodate the dyes (cf. Table 1).

Table 2. Apparent binding constants (K_a) and binding stoichiometries (n) of dyes **1a–b** and **2b** to quadruplex and duplex oligonucleotides, determined from fluorimetric titrations.[a]

	1a		**1b**		**2a**	
DNA	n	K_a / 10^6 M^{-1}	n	K_a / 10^6 M^{-1}	n	K_a / 10^6 M^{-1}
22AG	2	0.47	2	0.93	2	0.17
c-myc	2	0.55	2	0.35	2	0.14
c-kit87up	1	0.31	1	0.36	2	0.20
c-kit2	0.5	0.76	0.5	0.70	2	0.24
TBA	1	0.13	1	0.27	1	0.21
ds-lac	2	0.12	2	0.67	2	8.91
DrewAT	1	0.09	1	0.68	1	18.4

[a] Experimental conditions: c(dye) = 2.5 μM in 10 mM $LiAsMe_2O_2$, 100 mM KCl buffer, pH 7.2. For calculation details see Experimental Part.

Competitive fluorimetric titrations. To confirm the selective fluorescence response of the dyes **1a** and **1b** binding to quadruplex DNA, we repeated the fluorimetric titrations of these dyes with the 22AG quadruplex in the presence of a large excess of duplex DNA (ct DNA, 200 μM bp). The results (Figure 7) showed that fluorimetric detection of quadruplex DNA is indeed possible in these conditions. Thus, although the fluorescence of the dyes was

affected by the presence of ct DNA, the addition of the quadruplex led to a much higher enhancement of fluorescence, demonstrating the displacement of the dyes from ct DNA and the formation of highly fluorescent complexes with the quadruplex. These results demonstrate the high potential of **1a** and **1b** to serve as quadruplex-sensitive fluorescent probes in the competitive biological environment.

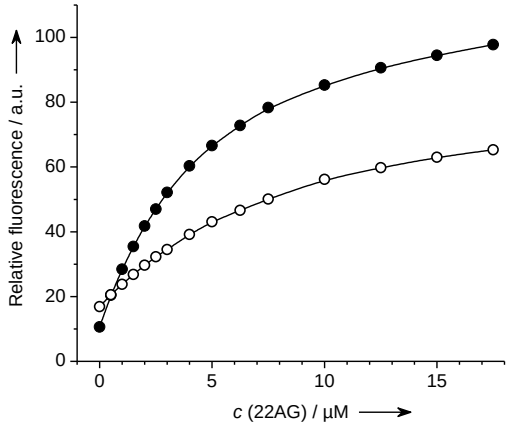

Figure 7. Spectrofluorimetric titrations of the 22AG quadruplex to the dyes **1a** (filled circles; λ_{ex} = 510 nm) and **1b** (empty circles; λ_{ex} = 519 nm) in the presence of excess ct DNA (200 μM bp). The concentration of the dyes was 2.5 μM in 10 mM $LiAsMe_2O_2$, 100 mM KCl buffer, pH 7.2. The fluorescence intensities are normalized with respect to the fluorescence of free dyes in the absence of 22AG and ct DNA.

Thermal denaturation experiments

To further study the binding affinities of the dyes to nucleic acids, we performed UV-monitored thermal denaturation experiments with the same set of structures. Although the well-established fluorescence-monitored thermal denaturation of double-labeled oligonucleotides ("FRET melting") is usually the method of choice for evaluation of affinity of quadruplex-DNA ligands,[23] we used UV-monitored denaturation to avoid any possible interference of the fluorescence of the dyes with the fluorophore-labeled oligonucleotides.[24] TMPyP4 (*meso*-tetra(*N*-methyl-4-pyridyl)porphine tosylate), the well-studied universal DNA ligand that binds with high affinity both to quadruplex and duplex DNA, was used as a reference.[25,26] The thermal denaturation data (Table 3) indicate that the distyryl dyes **1a–b** and **2a** greatly differ in their propensity to stabilize duplex and quadruplex nucleic acids. Thus, the dyes **1a** and **1b** displayed moderate to high stabilization of most quadruplex structures, with the largest stabilization observed for c-myc and c-kit2 (**1a**: ΔT_m = 11.3 and 9.4 °C, **1b**: ΔT_m = 15.0 and 13.9 °C, respectively). Consistently with the previous data, **1a** and **1b** induce small to negligible effects on the melting temperature of TBA and the ds-lac duplex (1 °C ≤ ΔT_m ≤ 2 °C). These results emphasize the potential of dyes **1a–b** to stabilize preferentially parallel-stranded quadruplexes c-myc and c-kit2 over the hybrid forms (22AG, c-kit87up) as well as their good selectivity over duplexes. In contrast to **1a–b**, the dye **2a** showed much weaker stabilization of all quadruplex structures (1.5 °C ≤ ΔT_m ≤ 6.3 °C) whereas it induces a slightly more pronounced stabilization of the duplex (ΔT_m = 3.0 °C), thereby confirming its lower affinity for quadruplexes and its lower capacity to discriminates between the various DNA structures.

Table 3. Ligand-induced shifts of melting temperatures of duplex and quadruplex DNAs (ΔT_m / °C) for the dyes **1a–b**, **2a**, and TMPyP4 from UV-monitored thermal denaturation experiments.[a]

DNA	T_m^0 / °C[b]	**1a**	**1b**	**2a**	TMPyP4
22AG	52.7	6.0	9.1	2.6	6.5
c-myc	73.0	11.3	15.0	6.3	> 22
c-kit87up	49.9	6.0	8.9	3.1	3.1
c-kit2	56.4	9.4	13.9	5.9	23.4
TBA	41.1	2.1	2.0	1.5	−2.4
ds-lac	68.8	0.9	2.0	3.0	8.1

[a] Experimental conditions: *c*(DNA) = 2 μM, *c*(dye) = 10 μM in K^+-rich buffer (10 mM $LiAsMe_2O_2$, 90 mM LiCl, 10 mM KCl, pH 7.2); λ = 260 nm for duplex and 295 nm for quadruplex DNA; estimated error ±1.0 °C. [b] Melting temperature in the absence of dyes.

Notably, the porphyrin TMPyP4 showed a trend similar to that of dyes **1a–b**, i.e. strong stabilization of parallel quadruplexes with a remarkably high value of ΔT_m for c-myc (> 22 °C) and weaker stabilization of hybrid form c-kit87up (ΔT_m = 3.1 °C). Again, we observed absence of binding and even destabilization of TBA (negative ΔT_m).[27] Although TMPyP4 is usually considered as a good quadruplex ligand, destabilization of certain quadruplex structures is not unprecedented.[28] The stabilization of duplex ds-lac is much higher (ΔT_m = 8.1 °C) than that induced by the distyryl dyes.

Of note, the quadruplex structures showed varying ligand-induced stabilization: the intrinsically very stable c-myc quadruplex (T_m^0 = 73.0 °C) was readily stabilized by **1a**, **1b** and TMPyP4, whereas the thermodynamically less stable c-kit87up and TBA (T_m^0 = 49.9 and 41.1 °C, respectively) generally underwent much smaller ligand-induced stabilization. Taken together the results indicate that the quadruplex matrices have different propensities to accommodate ligands, while the latters, in turn, may interact differently with the structural features of the quadruplexes (grooves, loops, G-quartets).

Gel staining experiments

The fluorescence enhancement observed upon the interactions of **1a** and **1b** with quadruplex DNA structures prompted us to investigate these dyes as fluorescent stains in native polyacrylamide gel electrophoresis (PAGE). It has been observed that quadruplex DNA is poorly visualized in native gel electrophoresis by common fluorescent stains such as ethidium bromide, GelRed™ or SYBR® Safe.[29–30] We observed that post-staining of PAGE gels with solutions of **1a** or **1b** (2 μM), followed by fluorescence detection at λ = 670 nm, selectively visualizes the bands corresponding to the telomeric quadruplex (22AG) and c-myc (**1a**: Figure 8, a; **1b**: Supporting Information, Figure S5, a). In contrast, almost no fluorescence was observed in the bands containing duplex DNAs (ds-lac, DrewAT) and TBA. In the case of c-kit2 and c-kit87up, several minor bands were observed along with a non-migrating band,

revealing the tendency of these sequences to form dimeric and/or multimeric structures. This is in agreement with the tendency of c-kit2 quadruplex to dimerization[31] and the unusual ligand : quadruplex stoichiometry observed in fluorimetric titrations.

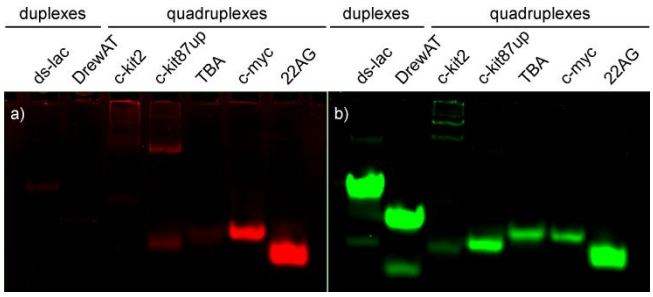

Figure 8. a) Gel electrophoresis of duplex and quadruplex nucleic acids (75 pmol per well) after staining with **1a** (2 μM in TBE buffer with 20 mM KCl). Excitation: 532 nm; detection: 670 nm (band-pass filter of 30 nm). b) The same gel additionally stained with TO (2 μM). Excitation: 532 nm; detection: 526 nm (short-pass filter). The fast-migrating bands in the ds-lac and DrewAT lanes correspond presumably to the intramolecular hairpin structures.

Moreover, we found that subsequent post-staining of the gel with TO (2 μM), followed by fluorescence detection at λ = 526 nm, allowed visualization of all bands due to the ability of TO to visualize the quadruplex and duplex DNA almost equally well (Figure 8, b). This two-dye staining protocol represents a simple and sensitive method for detection and discrimination of quadruplex and duplex DNA structures in gel electrophoresis. In a separate experiment, as little as 5 pmol/well of 22AG quadruplex could be detected, with **1b** and TO showing comparable sensitivity (Supporting Information, Figure S6). This highlights the potential of distyryl dyes **1a** and **1b** to be used as quadruplex-selective fluorescent stains.

In contrast, staining of the gel with **2a** (2 μM) selectively revealed the bands corresponding to ds-lac and DrewAT duplexes, in full agreement with the high affinity of **2a** to these oligonucleotides (Supporting Information, Figure S5, b).

Discussion and conclusion

Structural aspects. In this work, we systematically studied the interaction of three distyryl dyes of the D–π–A^+–π–D architecture (D = electron-donating 4-(dimethylamino)phenyl group, A = electron-accepting pyridinium unit) with a number of quadruplex and duplex nucleic acids. The comparison of the substitution isomers **1a** and **2a** allowed us to study the influence of geometry of the dye on their DNA-binding properties. The comparison of **1a** with **1b** revealed the impact of the chain and its additional positive charge on the quadruplex- and duplex-DNA-binding properties. Moreover, the position of the *N*-methyl substituent in **1a** and **2a** is different with respect to the chromophore: in **1a** it points outwards from the arc-shaped chromophore, whereas in **2a** it points inwards the crescent-shaped molecule. Indeed, the single-crystal X-ray diffraction study of **1a** and **2a** (Figure 1) showed that, in the solid state, these isomers have different mutual orientations of the phenylstyryl groups, leading to different size and geometry of the chromophores. The X-ray studies also revealed significant flexibility of the distyryl chromophore which, in spite of its double-bond-conjugated character, experiences torsion of up to 30.8° in **2a**; interestingly, this deviation of planarity was also reproduced in quantum chemical calculations. However, the other recently-published solid-state structure of **2a** in a crystal obtained from a different solvent (DMSO) showed a much smaller degree of non-planarity (torsion of the styryl substituents by only 9.5° and 5.7°, respectively).[16b] Altogether, this indicates that the scaffold of distyryl dyes has some plasticity that enables adaptation to the environment, such as the packing motif in the solid state or steric clashes upon binding to biomolecular targets.

Binding to quadruplex and duplex nucleic acids. Globally, the two methods (fluorimetric titrations and thermal denaturation) show good agreement with respect to binding affinities of the dyes for their DNA targets, and lead to the following conclusions: (i) The 2,4-distyryl dyes **1a** and **1b** bind to most quadruplex DNA (except for TBA) with a rather high affinity, as supported by the values of the binding constants (K_a = 0.31–0.93 × 10^6 M^{-1} from fluorimetric titrations) and thermal denaturation data (ΔT_m = 6–15 °C). All data also demonstrate that both compounds have higher affinity towards c-myc and c-kit2 quadruplexes, compared with 22AG and c-kit87up. Nevertheless, the highest fluorescence increase (80–100-fold) is observed upon binding of dyes to the human telomeric quadruplex 22AG. This highlights the fact that the experimentally observed fluorescence increase is a product of the binding constant and the fluorescence quantum yield of the dye bound to its target DNA, which are not interrelated entities. Thus, the remarkable fluorescence enhancement of both dyes in complex with 22AG is presumably due to a binding interaction or an environment which are different from the other quadruplexes. (ii) Dyes **1a–b** have a particularly low affinity for duplex DNA, as evidenced by the two methods and are poorly fluorescent when bound to this structure. In this regard, spectrophotometric titrations demonstrate that duplex DNA templates the formation of J-aggregates of the dye **1a**, which is intrinsically prone to aggregation (cf. Figure 4, a). DNA-induced formation of dye aggregates is not unprecedented, as H- and J-type aggregates of cyanine dyes formed on a DNA template have been described.[32] However, the relationship between the affinity of aggregated dye towards duplex DNA and the stabilization of the duplex structure has not been addressed. It may be expected that the unfavorable shape of J-aggregates causes them to bind only weakly and thus do not significantly contribute to the thermal stabilization of the duplex. In contrast, introduction of a cationic aminoalkyl chain in **1b** prevents the aggregation in aqueous medium and increases affinity to quadruplex and, to a smaller extent, duplex nucleic acids, leading to slightly lower optical selectivity (cf. Figure 7). (iii) The properties of the symmetric dye **2a** are very different from its asymmetric counterpart. The two employed methods give evidence that the affinities of **2a** to all quadruplex DNAs are significantly lower than those of **1a**–**b**; meanwhile, **2a** has high affinity for double-stranded targets. The latter is especially pronounced in the case of DrewAT duplex, as shown by the results of fluorimetric titrations (K_a = 18.4 × 10^6 M^{-1}). This duplex features an AAATTT sequence, well-suited for accommodation of groove-binding ligands,[10d,33] and it may be argued that high affinity of **2a** to this structure is due to a well-defined minor groove-binding mode.

Altogether, these observations highlight the importance of the geometry of distyryl dyes for their binding to nucleic acids. Thus, the asymmetric dyes **1a** and **1b** may be described as quadruplex-DNA ligands with good affinity and fair quadruplex-vs.-duplex binding selectivity [K_a(G4) / K_a(ds) ≈ 2.5–8]. However, both dyes display excellent optical selectivity, i.e. specific fluorescence enhancement in upon binding to quadruplex DNA, and particularly

to the human telomeric quadruplex. On the contrary, in spite of relatively small structural differences, the symmetric analogue **2a** has a several-fold lower affinity for quadruplex structures than **1a–b,** and does not discriminate between different DNA structures by its fluorescence response. Notably, the dye **2a** is closely similar to 2,6-bis(4-methylthiostyryl)-1-methylpyridinium (C61), a green-emitting fluorescent probe for double-stranded DNA recently identified by screening, which differs only by the nature of electron-donor substituents.[12]

Finally, binding of distyryl dyes to quadruplex DNAs also depends strongly on the various quadruplex matrices. Thus, all dyes bind with a 2 : 1 or 1 : 1 (ligand : quadruplex) stoichiometry to 22AG, c-myc and c-kit87up quadruplexes, in agreement with literature data for other ligands.[34,35] On the other hand, both **1a** and **1b** bind to the c-kit2 quadruplex with an apparent 1 : 2 stoichiometry. This observation may be explained by the high propensity of the c-kit2 quadruplex to dimerization,[31] which provides a ligand binding site at the interface between monomeric units.[36] However, it cannot be deduced whether the ligand binds to the quadruplex dimers existing in solution or induces dimerization. Finally, worth mentioning is the poor ability of the TBA quadruplex to bind the distyryl compounds, as evidenced from the small binding constants and low ligand-induced stabilization. This could reveal a binding mode outside the G-quartets, as TBA was shown to readily accommodate planar aromatic ligands[37] but not ribbon-like molecules which are likely to interact with the grooves.[38]

Potential as fluorescent probes for quadruplex DNA and comparison with existing probes. The distyryl dyes have favorable spectral properties for using them as optical probes: they emit in the far red region of the visible spectrum and have large Stokes shifts of up to 200 nm, which allow good spectral separation from the excitation light and reduce the background signal in analytical applications. The high optical selectivity of **1a** and **1b** for quadruplex DNA and, in particular, the human telomeric quadruplex, makes these dyes good candidates as quadruplex-selective fluorescent probes, as shown by the successful fluorimetric detection of 22AG in the presence of a large excess of competing double-stranded DNA and in gel electrophoresis. Interestingly, the results obtained in gel staining experiments parallel the solution data: 22AG and c-myc quadruplexes, which aptly migrate in gel electrophoresis, are very well visualized with **1a** and **1b**, while the TBA quadruplex and both duplexes are poorly or not detected. On the contrary, staining with **2a** reveals the duplex structures exclusively, due to the high affinity of this dye to duplex DNA.

The optical quadruplex-vs.-duplex selectivity of distyryl dyes **1a** and **1b** is comparable to those of pyridodicarboxamide–thiazole orange conjugate (PDC-M-TO), described earlier by our group;[8] however, the latter showed a much stronger propensity to aggregate in aqueous solutions, disfavorable for practical applications. The recently reported benzothiazole–benzofuroquinolinium dye displays higher fluorescence enhancements (~ 300–350-fold in the presence of quadruplex DNA)[7] than **1a–b**; however, a significant advantage of distyryl dyes is their large Stokes shift, allowing good optical separation of the excitation light and leading to lower background fluorescence. Finally, another well-studied quadruplex-DNA probe with a styryl scaffold, BMCV, has no strong preference for quadruplex vs. duplex DNA in terms of binding affinity or fluorescence enhancement, but can discriminate between them by modulation of other photophysical properties such as fluorescence lifetime and emission wavelength.[14] In the case of distyryl dyes **1a–b**, it is likely that the differences in characteristics of binding site(s) (hydrophobicity, polarity, orientation of the dye with respect to nucleic acid bases) between duplex and quadruplex DNA result in the formation of weakly- and strongly-fluorescent complexes, respectively.

In conclusion, given that dyes **1a** and **1b** have favorable spectral properties and are readily available, it may be expected that they could successfully complement the set of quadruplex "light-up" probes reported to date[3] and would find applications as quadruplex-selective fluorescent DNA probes in solution and gel electrophoresis experiments.

Experimental Section

General remarks: All commercially available chemicals, used for synthesis, were reagent grade and used without further purification. NMR spectra were measured with a Bruker Avance 300 (^{1}H: 300 MHz, ^{13}C: 75 MHz) spectrometer at 25 °C; chemical shifts are given in ppm (δ) values (internal standard TMS). Multiplicities of ^{13}C NMR signals were determined by means of DEPT-135 experiments. The melting points were determined in open-end capillaries with a digital melting point instrument (SMP30, Stuart). Elemental microanalyses of the new compounds were performed by the *Service de Microanalyse*, CNRS–ICSN, Gif-sur-Yvette, France. Mass spectra (ESI in the positive-ion mode) were recorded with a Waters ZQ instrument (source voltage 50–75 kV). The degree of purity of the dyes was verified by HPLC analysis (Waters Alliance 2525 equipped with a Waters XTerra MS C_{18}-5 µm column and Waters 2996 photodiode array detector; eluent A: water with 0.1% HCOOH, eluent B: MeCN, gradient elution with 10 to 100% of eluent B). Oligonucleotides (see sequences in Table 2), purified by RP-HPLC, were purchased from Eurogentec. Calf thymus DNA solution (10 mg mL^{-1}) was purchased from Invitrogen.

Synthesis of dyes: The dyes **1a** and **2a** were prepared in 90–95% yield according to the published procedures[18] and gave satisfactory ^{1}H and ^{13}C NMR, MS and elemental analysis data.

2,4-Dimethyl-1-(4-(triethylammonio)butyl)pyridinium dibromide (3): A mixture of (4-bromobutyl)triethylammonium bromide[39] (2.74 g, 8.65 mmol) and 2,4-lutidine (1.00 mL, 0.927 g, 8.65 mmol) in MeCN (25 mL) was heated under reflux for 22 h. After cooling to room temperature, the white precipitate was collected, washed with MeCN and dried, to afford **3** (2.20 g, 60%) as a white solid, m.p. 208–209 °C; ^{1}H NMR ([D$_6$]DMSO): δ = 1.19 (t, J = 7 Hz, 9H), 1.74 (m, 2H), 1.87(m, 2H), 2.55 (s, 3H), 2.82 (s, 3H), 3.27–3.19 (m, 8H), 4.57 (t, J = 7 Hz, 2H), 7.84 (d, J = 6 Hz, 1H), 7.93 (s, 1H), 8.98 (d, J = 6 Hz, 1H); ^{13}C NMR ([D$_6$]DMSO): δ = 7.3 (CH_3), 18.3 (CH_2), 19.5 (CH_3), 21.1 (CH_3), 26.4 (CH_2), 52.2 (CH_2), 55.4 (CH_2), 55.7 (CH_2), 126.1 (CH), 130.1 (CH), 144.4 (CH), 154.0 (C_q), 158.2 (C_q); MS (ESI$^+$): m/z (%) = 132.7 (100) $[M]^{2+}$, 263.3 (47) $[M - H]^+$, 343.4 (60) $[M + Br]^+$.

2,4-Bis((*E*)-4-(dimethylaminostyryl)-1-(4-(triethylammonio)butyl)pyridinium dibromide (1b): A mixture of **3** (0.424 g, 1.00 mmol), 4-(dimethylamino)benzaldehyde (0.448 g, 3.00 mmol) and piperidine (0.198 mL, 2.00 mmol) in EtOH (25 ml) was heated under reflux for 6 h. After cooling to room temperature, the red precipitate was collected by filtration and recrystallized from EtOH, to afford **1b** as red microcrystalline solid (0.410 g, 60%), m.p. 236–237 °C; ^{1}H NMR ([D$_6$]DMSO): δ = 1.18 (t, J = 7 Hz, 9H); 1.77–1.85 (m, 4H), 3.02 (s, 6H), 3.03 (s, 6H), 3.20–3.28 (m, 8H), 4.67 (t, J = 7 Hz, 2H), 6.80 (m, 4H), 7.16 (d, J = 16 Hz, 1H), 7.23 (d, J = 16 Hz, 1H), 7.60 (d, J = 9 Hz, 2H), 7.77 (d, J = 9 Hz, 2H), 7.83 (dd, J = 7.0 Hz, J = 2 Hz, 1H), 7.95 (d, J = 16 Hz, 1H), 7.97 (d, J = 16 Hz, 1H), 8.42 (d, J = 2 Hz, 1H), 8.63 (d, J = 7 Hz, 1H); ^{13}C NMR ([D$_6$]DMSO): δ = 7.4 (CH_3), 18.4 (CH_2), 26.7 (CH_2), 52.5 (CH_2), 55.4 (CH_2), 55.7 (CH_2), 110.9 (CH), 112.0 (CH), 112.2 (CH), 117.8 (CH), 118.8 (CH), 119.7 (CH), 122.7 (C_q), 122.9 (C_q), 130.2 (CH), 130.8 (CH), 141.2 (CH), 143.6 (CH), 143.9 (CH), 151.9 (C_q), 152.0 (C_q), 152.2 (C_q), 152.4 (C_q); MS (ESI$^+$): m/z (%) = 263.3 (100) $[M]^{2+}$; elemental analysis calcd (%) for $C_{35}H_{50}Br_2N_4 \times 0.5\ H_2O$: C, 60.43; H, 7.39; N, 8.05; found: C, 60.44; H, 7.63; N, 7.99; purity (LC/MS): > 99%.

X-ray crystallography: Crystals of **1a** and **2a**, suitable for X-ray diffraction analysis, were obtained by recrystallization from MeCN–H_2O. Details of the crystal data, data collection and refinement are given in Table S1 (Supporting Information). The diffraction intensities were collected with graphite-monochromatized Mo $K\alpha$ radiation. Data collection and cell refinement were carried out using a Bruker Kappa X8 APEX II diffractometer. The temperature of the crystal was maintained at 100 K by means of a 700 series Cryostream cooling device with an accuracy of ±1 K. Intensity data were corrected for Lorenz polarization and absorption factors. The structures were solved by

direct methods using SHELXS-97[40] and refined against F^2 by full-matrix least-squares methods using SHELXL-97[41] with anisotropic displacement parameters for all non-hydrogen atoms. All hydrogen atoms were localized in difference Fourier maps and introduced into the calculations as a riding model with isotropic thermal parameters. All calculations were performed using the crystallographic software package WinGX.[42] The structures were drawn with ORTEP-3. CCDC-887388 (**1a**) and CCDC-887389 (**2a**) contain the supplementary crystallographic data for this paper. These data can be obtained free of charge from the Cambridge Crystallographic Data Centre via www.ccdc.cam.ac.uk/data_ request/cif.

Spectrophotometric and spectrofluorimetric titrations: Stock solutions (4 mM) of the dyes were prepared in DMSO (**1a**, **2a**) or 50% v/v DMSO–water (**1b**). Spectrophotometric and spectrofluorimetric titrations of dyes with oligonucleotides or ct DNA were performed in 10 mM $LiAsMe_2O_2$, 100 mM KCl buffer (pH 7.2). Absorption spectra were recorded with an Agilent 300 Bio double-beam spectrophotometer in quartz cells (path length 1 cm), using slit widths of 2 nm and scan rates of 200 to 600 nm min^{-1}. Fluorescence spectra were recorded with a HORIBA Jobin–Yvon FluoroMax-3 fluorimeter in quartz cells with a cross-section of 1 × 0.5 cm, using slit widths of 2 nm and integration time of 0.1–0.5 s. The excitation wavelengths for fluorimetric titrations corresponded to the isosbestic points found from the preliminary spectrophotometric titrations. The data from fluorimetric titrations were analyzed according to the independent-site model[22] by non-linear fitting to the equation

$$F / F_0 = 1 + \frac{(Q-1)}{2}\left(A + x + 1 - \sqrt{(A + x + 1)^2 - 4x}\right),$$

where F_0 is integral fluorescence intensity in the absence of DNA; Q is the fluorescence enhancement upon saturation, $A = [K_a \times c(\text{dye})]^{-1}$ and $x = c(\text{DNA}) \times n / c(\text{dye})$; n is the putative number of binding sites on a given DNA matrix. The parameters Q and A were found by Levenberg–Marquardt fitting routine in Origin 8.5 software, while n was varied to obtain a better fit.

Thermal denaturation experiments: The thermal denaturation profiles were recorded as described[24] on an Agilent 300 Bio spectrophotometer equipped with a Peltier-controlled multicell holder. Prior to measurements, the samples containing 2 µM oligonucleotides in 10 mM $LiAsMe_2O_2$, 90 mM LiCl, 10 mM KCl buffer (pH 7.2) were heated to 90 °C, kept for 5 min, cooled to room temperature, and the stock solution of dyes were added to final concentration of 10 µM. The measurement cycle involved cooling from ambient temperature to 10 °C, keeping at 10 °C for 2 min, heating to 95 °C at a rate of 0.2 deg min^{-1}, and cooling to 20 °C at 0.4 deg min^{-1}. The absorbance was monitored at 295 nm (for quadruplex DNA) or 260 nm (for duplex DNA) during the heating and cooling ramps. The temperatures of DNA melting transitions (T_m) were determined from the first-derivative plots of absorbance versus temperature.

Native PAGE experiments: Gel electrophoresis was performed using 16% (19:1) poly-acrylamide gels (160 × 140 × 0.75 mm). 75 pmol of various duplex- and quadruplex-forming oligonucleotides (see sequences in Table 2) were run in 1X TBE buffer (89 mM Tris–borate, 2 mM EDTA, pH 8.3) supplemented with 20 mM KCl, using the following parameters: temperature, 8 °C; voltage, 150 V; time, about 5 h. Post-staining was performed with a mixture of **1a** or **1b** (0.5 µM) and TO (0.5 µM) in 1X TBE buffer containing 20 mM KCl. Gels were scanned with a Typhoon Trio (GE Healthcare) using the following parameters: excitation wavelength, 532 nm; detection, 526 nm short-pass filter (TO) or 670 nm / 30 nm band-pass filter (**1a** and **1b**); PMT voltage, 600 V; resolution, 100 µm.

Quantum chemical calculations: The geometries of **1a** and **2a** (in the conformations corresponding to those found in the solid state) were fully optimized using DFT calculations with a hybrid exchange-correlation CAM-B3LYP functional and a D95V basis set, as implemented in Gaussian 03 program.[43] The ground-state optimized geometries were used for TD-DFT calculations, on the same level of theory, of molecular orbitals and electronic transitions. The electron density was analyzed according to the Merz–Singh–Kollman scheme and visualized with Molekel.[44] Excited-state dipole moments and electron densities were calculated using the one-particle RhoCI density. The default Gaussian 03 parameters were used in every case.

Acknowledgements

This research was financially supported by the Centre National de la Recherche Scientifique. B.C. thanks the MIT–France program for her summer internship. We thank Dr. Yuliya Sedletska (Institut Curie) for help with gel electrophoresis experiments.

[1] J. L. Huppert, *Chem. Soc. Rev.* **2008**, *37*, 1375–1384

[2] H. J. Lipps, D. Rhodes, *Trends Cell Biol.* **2009**, *19*, 414–422.

[3] E. Largy, A. Granzhan, F. Hamon, D. Verga, M.-P. Teulade-Fichou, *Top. Curr. Chem.* **2012**, in press (DOI: 10.1007/128_2012_346).

[4] M. Tera, K. Iida, K. Ikebukuro, H. Seimiya, K. Shin-ya, K. Nagasawa, *Org. Biomol. Chem.* **2010**, *8*, 2749–2755.

[5] E. Largy, F. Hamon, M.-P. Teulade-Fichou, *Methods* **2012**, in press (DOI: 10.1016/j.ymeth.2012.02.008).

[6] H. Arthanari, S. Basu, T. L. Kawano, P. H. Bolton, *Nucleic Acids Res.* **1998**, *26*, 3724–3728.

[7] Y.-J. Lu, S.-C. Yan, F.-Y. Chan, L. Zou, W.-H. Chung, W.-L. Wong, B. Qiu, N. Sun, P.-H. Chan, Z.-S. Huang, L.-Q. Gu, K.-Y. Wong, *Chem. Commun.* **2011**, *47*, 4971–4973.

[8] P. Yang, A. De Cian, M.-P. Teulade-Fichou, J.-L. Mergny, D. Monchaud, *Angew. Chem. Int. Ed.* **2009**, *48*, 2188–2191.

[9] T. Deligeorgiev, A. Vasilev, S. Kaloyanova, J. J. Vauero, *Color. Technol.* **2010**, *126*, 55–80.

[10] a) C. Allain, F. Schmidt, R. Lartia, G. Bordeau, C. Fiorini-Debuisschert, F. Charra, P. Tauc, M.-P. Teulade-Fichou, *ChemBioChem* **2007**, *8*, 1439–4227; b) R. Lartia, C. Allain, G. Bordeau, F. Schmidt, C. Fiorini-Debuisschert, F. Charra, M.-P. Teulade-Fichou, *J. Org. Chem.* **2008**, *73*, 1732–1744; c) G. Bordeau, R. Lartia, G. Metge, C. Fiorini-Debuisschert, F. Charra, M.-P. Teulade-Fichou, *J. Am. Chem. Soc.* **2008**, *130*, 16836–16837; d) B. Dumat, G. Bordeau, E. Faurel-Paul, F. Mahuteau-Betzer, N. Saettel, M. Bombled, G. Metgé, F. Charra, C. Fiorini-Debuisschert, M.-P. Teulade-Fichou, *Biochimie* **2011**, *93*, 1209–1218; e) B. Dumat, G. Bordeau, A. I. Aranda, F. Mahuteau-Betzer, Y. El Harfouch, G. Metgé, F. Charra, C. Fiorini-Debuisschert, M.-P. Teulade-Fichou, *Org. Biomol. Chem.* **2012**, *10*, 6054–6061.

[11] Reviews: a) N. S. Finney, *Curr. Opin. Chem. Biol.* **2006**, *10*, 238–245; b) J.-S. Lee, Y. K. Kim, M. Vendrell, Y.-T. Chang, *Mol. BioSyst.* **2009**, *5*, 411–421.

[12] S. Feng, Y. K. Kim, S. Yang, Y.-T. Chang, *Chem. Commun.* **2010**, *46*, 436–438.

[13] E. Maçôas, G. Marcelo, S. Pinto, T. Cañeque, A. M. Cuadro, J. J. Vaquero, J. M. G. Martinho, *Chem. Commun.* **2011**, *47*, 7374–7376.

[14] a) C.-C. Chang, J.-Y. Wu, C.-W. Chien, W.-S. Wu, H. Liu, C.-C. Kang, L.-J. Yu, T.-C. Chang, *Anal. Chem.* **2003**, *75*, 6177–6183; b) C.-C. Chang, I.-C. Kuo, I.-F. Ling, C.-C. Chen, H.-C. Chen, P.-J. Luo, J.-J. Lin, T.-C. Chang, *Anal. Chem.* **2004**, *76*, 4490–4494; c) C.-C. Chang, J.-F. Chu, F.-J. Kao, Y.-C. Chiu, P.-J. Lou, H.-C. Chen, T.-C. Chang, *Anal. Chem.* **2006**, *78*, 2810–2815.

[15] **1a**: G. R. Clemo, G. A. Swan, *J. Chem. Soc.* **1938**, 1454–1455; **2a**: G. B. Crippa, T. Verdi, *Ann. Chim. Appl.* **1936**, *26*, 418–423.

[16] a) F.-Y. Hao, P .-F. Shi, H.-J. Liu, J.-Y. Wu, J.-X. Yang, Y.-P. Tian, G.-Y. Zhou, M.-H. Jiang, H. K. Fun, C. Suchada, *Chin. J. Chem.* **2004**, *22*, 354–359; b) X. Xu, W. Qiu, Q. Zhou, J. Tang, F. Yang, Z. Sun, P. Audebert, *J. Phys. Chem. B* **2008**, *112*, 4913–4917.

[17] C. G. Fortuna, V. Barresi, C. Bonaccorso, G. Consiglio, S. Failla, A. Trovato-Salinaro, G. Musumarra, *Eur. J. Med. Chem.* **2012**, *47*, 221–227.

[18] M. Matsui, S. Kawamura, K. Shibata, H. Muramatsu, *Bull. Chem. Soc. Jpn.* **1992**, *65*, 71–74.

[19] F. Würthner, T. E. Kaiser, C. R. Saha-Möller, *Angew. Chem.* **2011**, *15*, 3436–3473; *Angew. Chem. Int. Ed.* **2011**, *50*, 3376–3410.

[20] H. Wang, R. Helgeson, B. Ma, F. Wudl, *J. Org. Chem.* **2000**, *65*, 5862–5867.

[21] T. Yanai, D. P. Tew, N. C. Handy, *Chem. Phys. Lett.* **2004**, *393*, 51–57.

[22] F. H. Stootman, D. M. Fisher, A. Rodger, J. R. Aldrich-Wright, *Analyst* **2006**, *131*, 1145–1151.

[23] a) J.-L. Mergny, J.-C. Maurizot, *ChemBioChem* **2001**, *2*, 124–132; b) D. Renčiuk, J. Zhou, L. Beaurepaire, A. Guédin, A. Bourdoncle, J.-L. Mergny, *Methods* **2012**, in press (DOI: 10.1016/j.ymeth.2012.03.020).

[24] J.-L. Mergny, L. Lacroix, *UV Melting of G-Quadruplexes. Curr. Protoc. Nucleic Acid Chem.* **2009**, *37*, 17.1.1–17.1.15.

[25] J. Ren, J. B. Chaires, *Biochemistry* **1999**, *38*, 16067–16075.

[26] E. Largy, F. Hamon, M.-P. Teulade-Fichou, *Anal. Bioanal. Chem.* **2011**, *400*, 3419–3427.

[27] This is in contrast to the data of M. del Toro, R. Gargallo, R. Eritja, J. Jaumot, *Anal. Biochem.* **2008**, *379*, 8–15, who showed stabilization of TBA by ΔT_m =

7 °C in the presence of 1 molar equiv. of TMPyP4. However, in spite of numerous attempts, we were unable to repoduce these data with our setup.

[28] M. J. Morris, K. L. Wingate, J. Silwal, T. C . Leeper, S. Basu, *Nucleic Acids Res.* **2012**, *40*, 4137–4145.

[29] a) F. Koeppel, J.-F. Riou, A. Laoui, P. Mailliet, P. B. Arimondo, D. Labit, O. Petitgenet, C. Hélène, J.-L. Mergny, *Nucleic Acids Res.* **2001**, *29*, 1087–1096; b) Z.-Y. Kan, Y. Lin, F. Wang, X.-Y. Zhuang, Y. Zhao, D.-W. Pang, Y.-H. Hao, Z. Tan, *Nucleic Acids Res.* **2007**, *35*, 3646–3653; c) G. W. Collie, G. N. Parkinson, S. Neidle, F. Rosu, E. De Pauw, V. Gabelica, *J. Am. Chem. Soc.* **2010**, *132*, 9328–9334.

[30] E. Largy, personal communication.

[31] V. Kuryavyi, A. T. Phan, D. J. Patel, *Nucl. Acids Res.* **2010**, *38*, 6757–6773.

[32] a) M. Wang, G. L. Silva, B. A. Armitage, *J. Am. Chem. Soc.* **2000**, *122*, 9977–9986; b) K. C. Hannah, B. A. Armitage, *Acc. Chem. Res.* **2004**, *37*, 845–853; c) A. L. Stadler, B. R. Renikuntla, D. Yaron, A. S. Fang, B. A. Armitage, *Langmuir* **2011**, *27*, 1472–1479.

[33] a) D. G. Brown, M. R. Sanderson, E. Garman, S. Neidle, *J. Mol. Biol.* **1992**, *226*, 481–490; b) M. I. Sánchez, O. Vázquez, J. Martínez-Costas, M. Eugenio Vázquez, J. L. Mascareñas, *Chem. Sci.* **2012**, *3*, 2383–2387.

[34] a) P. S. Shirude, E. R. Gillies, S. Ladame, F. Godde, K. Shin-ya, I. Huc, S. Balasubramanian, *J. Am. Chem. Soc.* **2007**, *129*, 11890–11891; b) J. Alzeer, N. W. Luedtke, *Biochemistry* **2010**, *49*, 4339–4348; c) I. Manet, F. Manoli, B. Zambelli, G. Andreano, A. Masi, L. Cellai, S. Ottani, G. Marconi, S. Monti, *Photochem. Photobiol. Sci*. **2011**, *10*, 1326–1337 ; d) K. J. Castor, J. Mancini, J. Fakhoury, N. Weill, R. Kieltyka, P. Englebienne, N. Avakyan, A. Mittermaier, C. Autexier, N. Moitessier, H. F. Sleiman, *ChemMedChem* **2012**, *7*, 85 – 94.

[35] J. Dai, M. Carver, L. H. Hurley, D. Yang, *J. Am. Chem. Soc.* **2011**, *133*, 17673–17680.

[36] N. H. Campbell, G. N. Parkinson, A. P. Reszka, S. Neidle, *J. Am. Chem. Soc.* **2008**, *130*, 6722–6724.

[37] D. Monchaud, C. Allain, H. Bertrand, N. Smargiasso, F. Rosu, V. Gabelica, A. De Cian, J. L. Mergny, M.-P. Teulade-Fichou, *Biochimie* **2008**, *90*, 1207–1223.

[38] F. Hamon, E. Largy, A. Guédin-Beaurepaire, M. Rouchon-Dagois, A. Sidibe, D. Monchaud, J.-L. Mergny, J.-F. Riou, C.-H. Nguyen, M.-P. Teulade-Fichou, *Angew. Chem.* **2011**, *123*, 8904–8908; *Angew. Chem. Int. Ed.* **2011**, *50*, 8745–8749.

[39] M. Lombardo, M. Chiarucci, C. Trombini, *Chem. Eur. J.* **2008**, *14*, 11288–11291.

[40] G. M. Sheldrick, *SHELXS-97, Program for Crystal Structure Solution*, University of Göttingen : Göttingen, Germany **1997**.

[41] G. M. Sheldrick, *SHELXL-97, Program for the refinement of crystal structures from diffraction data*, University of Göttingen: Göttingen, Germany **1997**.

[42] L. J. Farrugia, *J. Appl. Cryst.* **1999**, *32*, 837–838.

[43] Gaussian 03, Revision C.01, M. J. Frisch, G. W. Trucks, H. B. Schlegel, G. E. Scuseria, M. A. Robb, J. R. Cheeseman, J. A. Montgomery, Jr., T. Vreven, K. N. Kudin, J. C. Burant, J. M. Millam, S. S. Iyengar, J. Tomasi, V. Barone, B. Mennucci, M. Cossi, G. Scalmani, N. Rega, G. A. Petersson, H. Nakatsuji, M. Hada, M. Ehara, K. Toyota, R. Fukuda, J. Hasegawa, M. Ishida, T. Nakajima, Y. Honda, O. Kitao, H. Nakai, M. Klene, X. Li, J. E. Knox, H. P. Hratchian, J. B. Cross, V. Bakken, C. Adamo, J. Jaramillo, R. Gomperts, R. E. Stratmann, O. Yazyev, A. J. Austin, R. Cammi, C. Pomelli, J. W. Ochterski, P. Y. Ayala, K. Morokuma, G. A. Voth, P. Salvador, J. J. Dannenberg, V. G. Zakrzewski, S. Dapprich, A. D. Daniels, M. C. Strain, O. Farkas, D. K. Malick, A. D. Rabuck, K. Raghavachari, J. B. Foresman, J. V. Ortiz, Q. Cui, A. G. Baboul, S. Clifford, J. Cioslowski, B. B. Stefanov, G. Liu, A. Liashenko, P. Piskorz, I. Komaromi, R. L. Martin, D. J. Fox, T. Keith, M. A. Al-Laham, C. Y. Peng, A. Nanayakkara, M. Challacombe, P. M. W. Gill, B. Johnson, W. Chen, M. W. Wong, C. Gonzalez, J. A. Pople, Gaussian, Inc., Wallingford, CT, **2004**.

[44] MOLEKEL 5.4.0.8, U. Varetto, Swiss National Supercomputing Centre, Manno (Switzerland), **2009**.

Received: ((will be filled in by the editorial staff))
Revised: ((will be filled in by the editorial staff))
Published online: ((will be filled in by the editorial staff))

Entry for the Table of Contents (Please choose one layout only)

Layout 1:

Catch Phrase

*Xiao Xie, Bina Choi, Eric Largy, Régis Guillot, Anton Granzhan, Marie-Paule Teulade-Fichou**

……...…… Page – Page

Asymmetric Distyrylpyridinium Dyes as Red-Emitting Fluorescent Probes for Quadruplex DNA

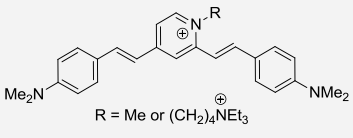

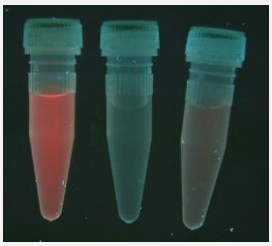

G4-DNA no DNA duplex DNA

Shape matters: the asymmetric (2,4-disubstituted) distyrylpyrydinium dyes represent red-emitting “light-up” fluorescent probes selective for quadruplex DNA, whereas their symmetric (2,6-disubstituted) counterpart has no selectivity for quadruplex over duplex DNA.